New capabilities of the INCL4.6
model implemented into high-energy transport codes

S. Leray[1], A. Boudard[1], B. Braunn[1], J. Cugnon[2], J.-Ch. David[1], A. Leprince[1], and D. Mancusi[1]

[1] CEA, Centre de Saclay, IRFU/SPhN, F-91191 Gif-sur-Yvette, France
[2] University of Liège, allée du 6 août 17, Bât. B5, B-4000 Liège 1, Belgium

Abstract

High-energy reactions in spallation targets produce a large number of radioactive isotopes that are a concern for radioprotection in normal conditions (gas release, waste disposal), in case of accident and in view of the decommissioning. Transport codes able to predict reliably the production of radioactive isotopes in spallation targets are therefore essential. Recently, the INCL4.6-Abla07 combination of models, which was proven to have a very good predictive power of spallation residue production in the IAEA benchmark of spallation models, has been implemented in a MCNPX2.7 and PHITS. Examples of simulations done with this code are presented. The first example concerns the European Spallation Source (ESS) tungsten target. A careful benchmarking of the code on W elementary cross-sections (excitation functions) allows assessing the uncertainty on the predictions of the most hazardous isotopes. The second one is devoted to the production of astatine (Z=85) isotopes in the ISOLDE (CERN) lead-bismuth target. Our model, thanks to the coalescence mechanism in the intranuclear cascade model and to an improved handling of low energy helium-induced reactions, correctly predicts the astatine yields. The recent extension of the model to light ion induced reactions and its implementation into GEANT4 is also discussed.

Introduction

The Liège Intranuclear Cascade model, INCL4 [1], has originally been developed to describe spallation reactions, i.e. nucleon and light charged particle induced collisions in the 100 MeV - 3 GeV energy range. The main motivations for the work on spallation reaction models were the development of spallation neutron sources, projects of accelerator-driven sub-critical reactors (ADS) that could be used to transmute long-lived radioactive waste and radioactive ion beam facilities. Other applications of high energy reactions involving also sometimes light-ion induced reactions are nowadays also raising a lot of interest: for instance hadrontherapy, radioprotection of astronauts and radiation damage to microelectronics circuits near accelerators or in space missions, and simulation of detector set-ups in nuclear and particle physics experiments. There is therefore a need for models, to be used in high energy transport codes, with a scope large enough to cover all these applications.

Coupled to the ABLA de-excitation code from GSI [2], INCL4 has been extensively compared with experimental data covering all possible reaction channels and continuously improved during the last ten years, part of the work being done in the framework of the HINDAS [3] FP5 and EUROTRANS/NUDATRA [4] FP6 EC projects, whose objective was to provide improved simulation tools for the design of ADS transmuters. The combination of versions developed in this framework, INCL4.5 [5] and ABLA07 [6], has been shown [7,8] to be one of the models giving the best overall agreement with experimental data in the benchmark of spallation models organized recently under the auspices of IAEA [9]. A new version, INCL4.6, very similar to INCL4.5 for nucleon-induced reaction above 100 MeV but improved for composite particle and energies below 100 MeV, has recently been released [10].

This version is now implemented into PHITS [11], in which it is coupled to the GEM de-excitation model. The same version, coupled to ABLA07, is available in a version of MCNPX [12]. A version fully re-written in C++, INCL++, extended to light-ion collisions up to ^{18}O has also been developed and is included into GEANT4 [13].

In this paper, we discuss the present capabilities of the new versions through comparisons with some elementary experimental data and examples of calculations with the model implemented into high-energy transport codes, in particular MCNPX and GEANT4, focussing on applications related to radioprotection and shielding issues.
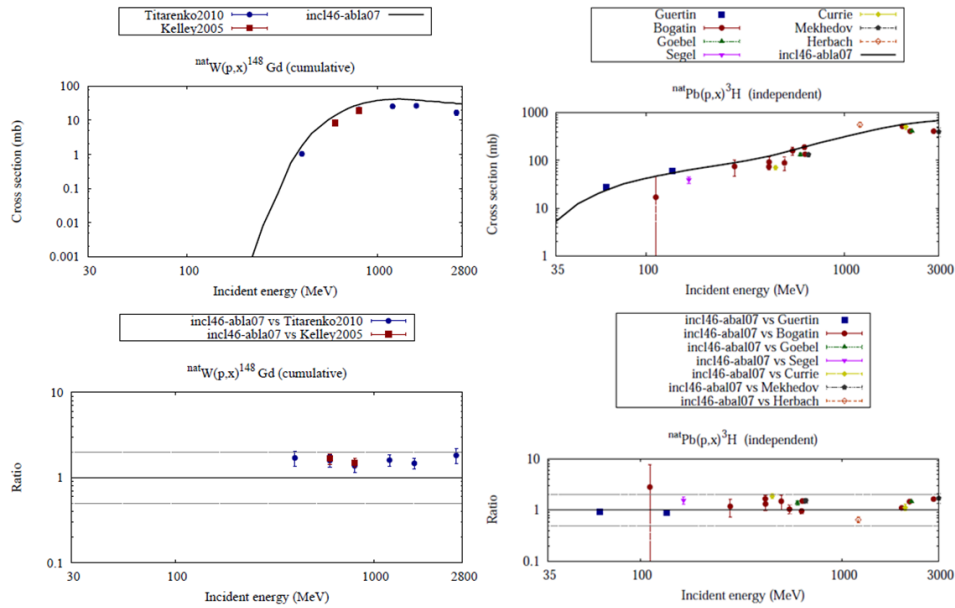
Simulations for the ESS target station

In the IAEA benchmark of spallation models, the main success of INCL4.5-ABLA07 compared the other participating models was encountered in the prediction of isotopic distributions of spallation residues. It is therefore likely that our model implemented into MCNPX will provide reliable calculations of spallation target radioactive inventories. An example of a simulation done recently with INCL4.6-ABLA07 implemented into MCNPX concerns the helium cooled, rotating tungsten target foreseen for the ESS facility, in which the radioactive inventory has been estimated and the major contributors to the radiotoxicity identified [14].

Validation of the model for the elementary reaction channels

Since the benchmark did not contain any experimental data on tungsten, we have first checked that our model gives a reasonable agreement on available excitation functions concerning isotopes appearing as main contributors to the radioactivity of the ESS target. Examples of such excitation functions are displayed in Figure 1 for some of most problematic nuclides for radioprotection, ^{148}Gd, which is an alpha emitter and tritium, which is a gas and therefore can easily escape. In all the cases where experimental data were available, the model reproduces data generally within a factor smaller than 2.

Figure 1: Experimental production cross sections of ^{148}Gd (left) and tritium (right) in p+W reactions compared with INCL4.6-Abla07 (lower part: ratio calculation/measurement). From [14].

Full simulation

The ESS target is composed by 11 tungsten layers of different thicknesses surrounded by 2 mm of helium [15]. The detailed geometry of the target and surrounding materials has been simulated with MCNPX and CINDER'90 has been used to take into account the production by low energy neutrons and decay of the different isotopes. In Figure 2, the activity at the end of an irradiation time of 3.6 years (left) and after a cooling time of 156 days (right), due to the different spallation products generated in the tungsten is represented on a chart of nuclides.

Figure 2: Nuclide activity (Bq) in the ESS tungsten target irradiated during 3.6 years, just after shut down (left), after 156 days off beam (right), obtained by INCL4.6-Abla07 in MCNPX+CINDER'90 on a chart of nuclides. From [14].
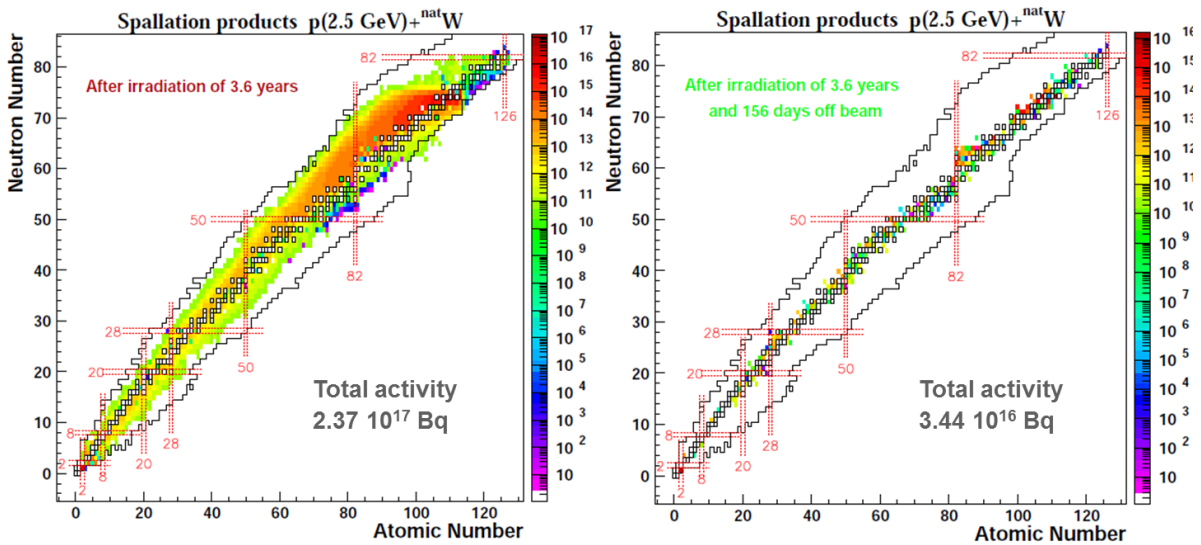
The left panel illustrates the very large number of radioactive nuclei produced in spallation reactions and the high level of the induced radioactivity. Although most of the generated nuclides are short-lived and have disappeared after 6 month (right panel) the total activity has only been reduced by a factor 6, mainly because it is due to a small number of major contributors, among which tritium.

As stressed in the preceding section, the fact that elementary reactions have been shown to be well predicted by our model gives confidence in the full simulation.

Production of astatine isotopes in the ISOLDE target

Recently, the IS419 experiment at the ISOLDE facility at CERN measured the production and release rates of volatile elements from a liquid lead-bismuth eutectic (LBE) target irradiated by a proton beam of 1 and 1.4 GeV [16]. Among others, the production of At isotopes was investigated. Although the production of astatine isotopes is relatively modest and these isotopes are generally short-lived, they could be a radioprotection issue since astatine is highly volatile and its isotopes decay to polonium isotopes. In [16], the experimental results were compared to simulations with different high energy transport codes, none of which were able to predict neither the order of magnitude of the measured astatine production nor the shape of the isotopic distribution. In [17], we have investigated astatine production channels in LBE and used our model in MCNPX to simulate the ISOLDE experiment.

Protons irradiating a LBE target can produce astatine isotopes through the following mechanisms: $^{209}Bi(p,\pi^-xn)^{210-x}At$, i.e. double charge exchange in primary reactions; secondary reactions induced by helium nuclei produced in primary collisions, $^{209}Bi(^3He,xn)^{212-x}At$ and $^{209}Bi(^4He,xn)^{213-x}At$. Contributions from other secondary reactions have been checked to be negligible. Actually, a first simulation of the ISOLDE experiment with MCNPX has revealed that isotopes with mass larger than 209 are produced only through secondary helium-induced reactions, ^4He playing a larger role and leading to higher masses. On the other hand, both mechanisms populate the other isotopes, the very lightest ones preferentially originating from double charge exchange reactions.

### *Validation of the model for the elementary reaction channels*

In order to estimate the reliability of our model regarding astatine production in LBE targets a careful validation on the involved elementary channels has been done. Concerning production of the light isotopes through double charge exchange reactions, the predictions of the model, not shown here, can be considered as correct within a factor of 2.

Since secondary reactions of helium nuclei play an important role, it is necessary to have a model able to correctly predict helium production in spallation reactions. In most models, helium is produced only in the de-excitation stage, which cannot account for the high-energy tail (above around 50 MeV) observed in the experimental spectra. Actually, only models having a specific mechanism to produce high-energy clusters of nucleons can aspire reproducing this tail. In INCL4, a mechanism based on surface coalescence in phase space has been introduced and leads to a very good agreement with experimental data all along the energy spectrum [10].

The treatment of secondary reactions induced by helium nuclei of energies below 100 MeV is also important. Although from the origin, the INCL4 model was designed to handle reactions with composite particle up to alpha, little attention had been paid to those up to recently. In addition, secondary reactions occur at low energies, generally below the alleged theoretical limit of validity of INC models. In the last version, the treatment of low-energy composite particle induced reactions has been significantly improved. Details of the modifications brought to the model are discussed in [10]. Let us just say here that the composite projectile is now described as a collection of off-shell independent nucleons with Fermi motion, ensuring full energy and momentum conservation and that a

phenomenological prescription has been added in order to lead to complete fusion at low energies. With these modifications, the model is able to predict rather well the helium-induced total reaction cross-sections and the individual channels, corresponding to the evaporation of x neutrons after fusion, which leads to the production of astatine nuclei, as can be seen in Figure 3.

Figure 3: ^{209}Bi(α,xn) (left) and ^{209}Bi(^{3}He,xn) (right) cross sections for x=1 to 6 as functions of the helium incident kinetic energy compared to the predictions of the INCL4.6+ABLA07 model. Experimental data come from the experimental nuclear reaction database EXFOR. From [17].
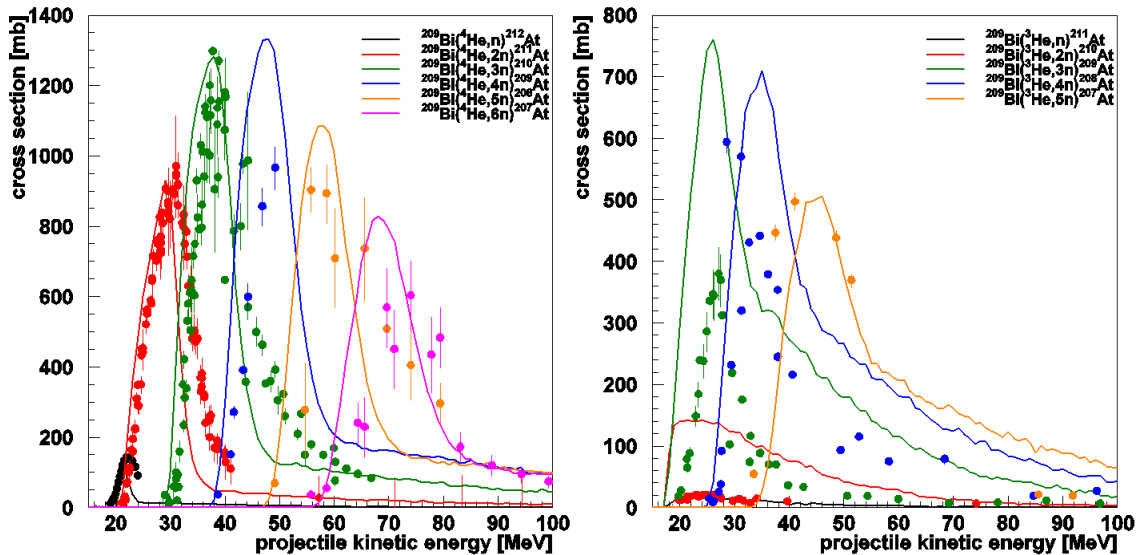
Actually, the situation is better in the case of ^{4}He than for ^{3}He, for which the x=1 and x=2 channels are largely overestimated, the agreement being restored only for the largest x values. However, in the ISOLDE target secondary reactions induced by ^{3}He are much less numerous than those due to ^{4}He for the channels with the smallest x-values. Since our model agrees well with the experimental data for ^{4}He for all x-values and for ^{3}He for x>2, we can expect the overall prediction to be reliable within a factor definitely smaller than 2.

Astatine production yields in the ISOLDE target

Figure 4 shows the result of the MCNPX simulation with INCL4.6-ABLA07 compared to the ISOLDE data at 1.4 GeV for the total production yields of astatine isotopes. An average release time from the liquid metal of 10 hours has been assumed during which the radioactive decay of the different isotopes is taken into account. A remarkable agreement between the calculation and the experiment is observed, regarding not only the shape of the isotopic distribution but also the absolute release rates. Clearly all the new features discussed in the preceding sections, in particular the better handling of low energy helium-induced reactions, have considerably improved the predictive capability of our model compared to the version used in [16].

In order to emphasize the importance of the secondary reactions induced by the clusters produced during the cascade stage through our coalescence mechanism, a calculation has been performed switching off this mechanism. The result is presented as the green curve and exhibits a severe deficit of heavy isotopes. Obviously, a model unable to emit high energy helium nuclei cannot be expected to correctly predict astatine production in a LBE target, since only a small fraction of the heliums produced in the evaporation stage have enough energy to undergo a reaction before being

stopped. This was the case of our first version INCL4.2, which is more or less mimicked by INCL4.6 without clusters, but also of the MCNPX default model option, Bertini-Dresner.

Figure 4: Astatine release rates from [16] at 1.4 GeV compared to MCNPX simulations, assuming an average release time of 10 hours, with INCL4.6-ABLA07 (red line), INCL4.6-ABLA07 in which the cluster production in the INC model was switched off (green line) and CEM03 (blue line). From [17].
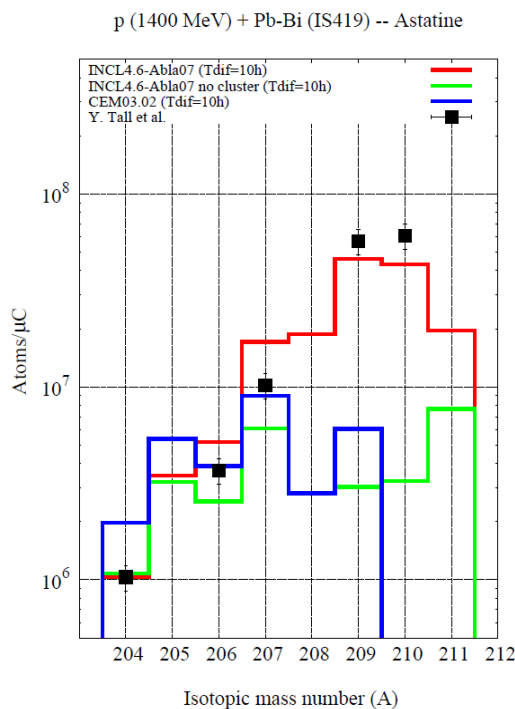
In the same figure, the results are also compared with CEM03 [18], which is also available in MCNPX2.7b (blue line), using the same assumption on the release time. It is interesting to note that this model is not able to account for the measured yield of the heavy astatine isotopes. In fact, CEM03 does have mechanisms to produce high-energy heliums but does not produce isotopes with mass larger than 209 probably because of an inappropriate treatment of low energy helium induced reactions.

This study on astatine isotopes suggests that the production of isotopes due to secondary reactions can easily be severely underestimated by usual models used in transport codes and that our model, thanks to the attention paid to the emission of high-energy clusters and to low-energy cluster induced reactions, can be considered as having a good predictive power for these isotopes.

Extension to light-ion induced reactions

The idea to extend our model to heavy-ion reactions has arisen from the need of predictive transport codes for applications such as hadrontherapy and protection against radiation in space or near accelerators. Since the model is very successful in nucleon and composite particle induced reactions, it seemed natural to try to extend it to heavier projectiles. It is clear however that our model cannot aspire to describe collisions of two very heavy nuclei since it does not have physics ingredients allowing for instance the prediction of important collective effects. Therefore, we have limited the extension to ^{18}O projectiles. The goal is to provide an event-generator for high-energy transport codes, able to calculate the characteristics of all particles and nuclei generated in a particular application, with a main focus on hadrontherapy.

The model

The first INCL light ion extension [19,20], based on the INCL4.2 version of the nucleon-induced reaction model, consisted of two main parts: handling of the projectile as a collection of individual nucleons and de-excitation of the projectile fragments after the reaction. The main cascade in the target nucleus is treated following the standard INCL cascade procedure as described in [1]. This version, translated to C++ and coupled with ABLA, has been included in GEANT4 [21]. In this approach, clearly the target and projectile are not treated symmetrically. If we try to interpret the reaction in the framework of a participant-spectator picture, the treatment of the target spectator and participant zone (where *NN* collisions happen) is satisfactory while the projectile spectator is obviously not correctly handled. When one is interested in fragments of the projectile, this deficiency is circumvented by reversing the reaction (i.e. the target impinging on the projectile) and then boosting it back to the laboratory frame.

Recently, the model has been revisited on the basis of the INCL4.6 version and totally rewritten in C++. This light-ion extended version is denoted as INCL++ and has been implemented in the latest GEANT4 beta release (v9.6 beta).

Let us briefly describe its main features. The projectile is described as a bulk of (N, Z) nucleons in the ion rest frame whose positions and momenta are randomly chosen in a realistic *r* and *p* space density (gaussian), with the constraint that the vectorial sum equal to zero in both spaces, and then Lorentz-boosted. For each configuration the depth of a binding potential is determined so that the sum of the nucleon energies is equal to the tabulated mass of the projectile nucleus. The nucleons are no more on mass shell but the sum of energies and vector momenta are correct. The ion follows globally a classical Coulomb trajectory until one of its nucleon impinges on a sphere of calculation around the target nucleus, large enough to marginally neglect nuclear interactions. Considering the collective cluster velocity, some of the nucleons will never interact with this sphere and will be combined together in the "projectile spectator". All other nucleons are entering the calculation sphere. They move globally (with the beam velocity) until one of them interacts, being close enough to a target nucleon. The *NN* interaction is then computed with the individual momenta, and Pauli blocking is tested. Nucleons crossing the sphere of calculation without any *NN* interaction are also combined in the "projectile spectator" at the end of the cascade.

The projectile spectator nucleus is kinematically defined by its nucleon content and its excitation energy obtained by an empirical particle-hole model based on the energy configuration of the current projectile and the removed nucleons (interacting with the target). This nucleus is then given to a de-excitation model. It is quite clear that this "projectile spectator" has not received any explicit contribution from the zone of interaction which is entirely contained in the target remnant with two consequences: the calculation is not symmetric and the residue of the target should be more realistic than the "projectile spectator" at this stage of the model. In this model, energy and momentum are always conserved.

Comparison with elementary experimental data

In order to compare with experimental data, the INCL++ model has to be coupled to a de-excitation model. Our standalone version has been coupled to the ABLA07 model [6], as the INCL4.6 fortran model. In GEANT4, it is linked with the native de-excitation handler [22]. This handler, depending on the mass and the excitation energy of the excited nuclei provided by the cascade, chooses between three different statistical de-excitation models (a Fermi break-up model, an evaporation model or a multifragmentation model) to bring back the nuclei to their fundamental state. This allows comparing the respective merits of ABLA07 and GEANT4 de-excitation.

- Neutron production

The calculation is still not symmetric although the projectile spectator is better treated than in the first version of our model. This means that, depending on the observable that one is interested in, the calculation should be done either in direct or in inverse kinematics. In Figure 5, left panel, we compare the model with neutron production cross-sections measured in the $^{12}C+^{12}C$ system at 290 MeV by Iwata et al. [25]. Calculations done using either inverse or direct kinematics are plotted. High energy neutrons in direct kinematics are mostly arising from *NN* collisions in the INC model plus neutrons from the de-excitation of the projectile spectator, while in inverse kinematics they result from the de-excitation of the target remnant or are the low energy partner in *NN* collisions. Globally the inverse kinematics gives a better agreement.

Figure 5: Neutron production double differential cross sections in the $^{12}C+^{12}C$ system at 290 MeV/u from [25] compared to INCL++ in GEANT4 in direct and inverse kinematics (left) and to the former version, INCL4.3 and BIC, all coupled to the GEANT4 de-excitation handler.
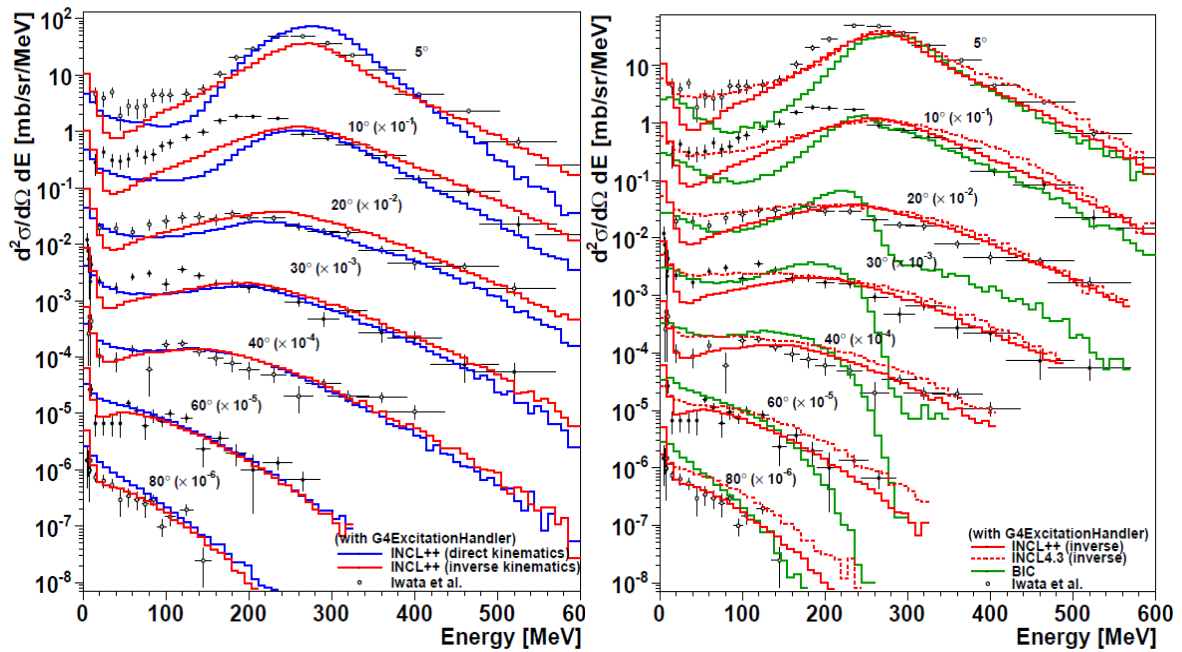

Figure 5, right panel, shows the comparison of the data with the present model, the former version INCL4.2, both in inverse kinematics, and to the binary cascade (BIC) from Folger et al. [23] also available in GEANT4, all models being coupled to the GEANT4 de-excitation handler. It can be observed that the new version of our model better reproduces the data than the former version and that BIC is definitely less good.

- Residue production

Results on residue production are generally more sensitive to details of the models than particle production. In Figure 7, top panels, several sets of data concerning charge changing cross-sections from [26] are compared to our model, present and former versions, and to BIC. All are linked to the GEANT4 de-excitation handler. The experiment was devoted to the study of iron projectile fragmentation on a carbon target. Since the model is available only up to oxygen projectiles, the calculations have been performed in inverse kinematics. As said before, we expect our model to be better for the target remnant, i.e. precisely for projectile fragments in inverse kinematics. Generally, our model gives a better agreement with the data than BIC. However, some significant discrepancies can be noticed, especially for the lightest residues.

Figure 6: Charge changing cross-sections in the Fe+C system at 3000 (left) and 500 MeV/u (right) from [26] compared with INCL++, INCL4.3 and BIC (top) and with INCL++ coupled to two different de-excitation models, ABLA07 and GEANT4 de-excitation handler.
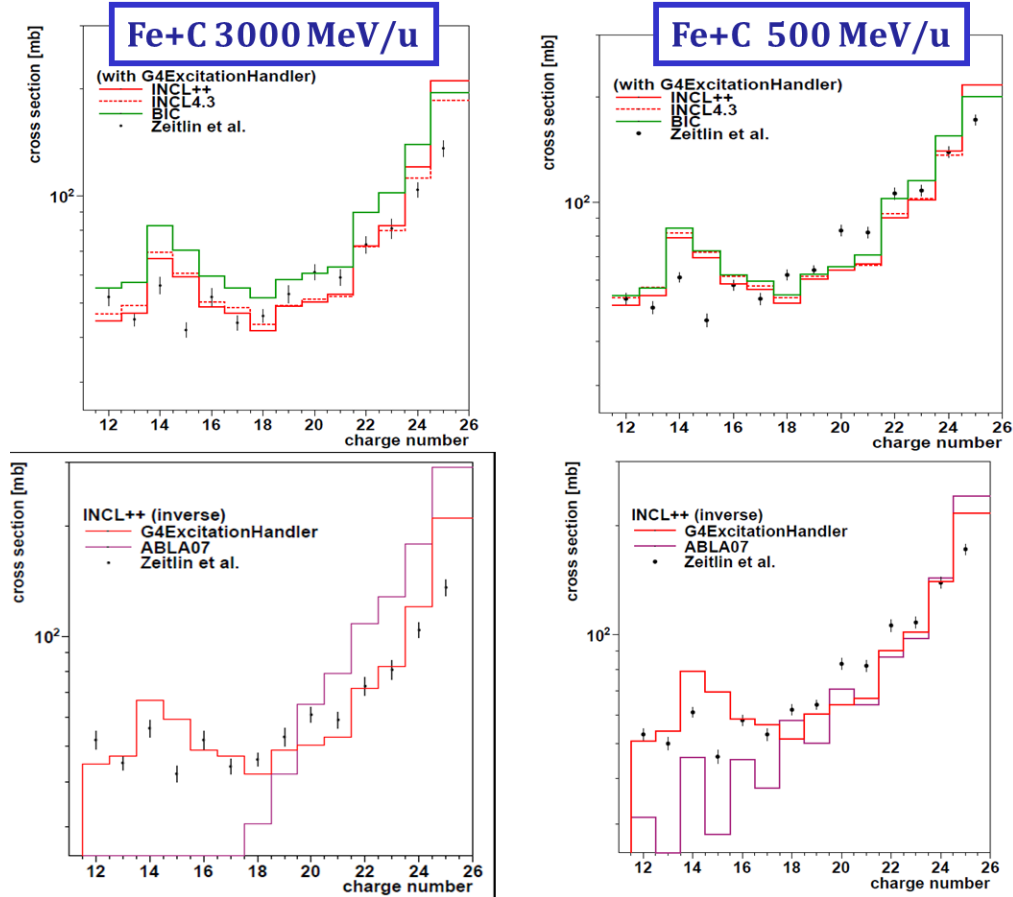

We have also compared the effect of the choice of the de-excitation model. This can be seen in Figure 7, bottom panels. Clearly the results are largely dependent on the choice: the GEANT4 de-excitation gives the best fit to the experimental data while ABLA07 has a problem in predicting light nuclei. This may be due to the fact that the model was up to now mainly tested, and therefore adjusted, on systems with excitation energies much smaller than the values reached in the cases studied here.

Comparison with thick target data

With the model implemented into GEANT4, it is possible to perform simulations of experiments done with thick targets. In Figure 7, data from B. Braunn et al. [27], in which nuclear charge distributions from the fragmentation of a ^{12}C beam at 95 MeV/u as projectile have been measured with different thicknesses of PMMA targets are presented. We here only show the comparison of production rates for the 5 mm target at three different angles.

It can be observed that our model reproduces rather well the light ion cross-sections (up to Z=4) but tends to underestimates higher charges at forward angles while BIC overestimates these elements at 10° and 20°. Calculations done with the GEANT4 Quantum Molecular Dynamic model (QMD) developed by Koi [24] are also shown and seems to give globally a slightly better agreement with the data. It should be stressed however that the CPU time needed to perform the simulation of the experiment is much longer in the case of QMD than with our model.

Figure 7: Nuclear charge distributions at different angles from a ^{12}C beam at 95 MeV/u interacting with a 5~mm PMMA target from [27] (red triangles) compared with INCL++ (blue crosses), BIC (blue circles) and QMD (blue squares).
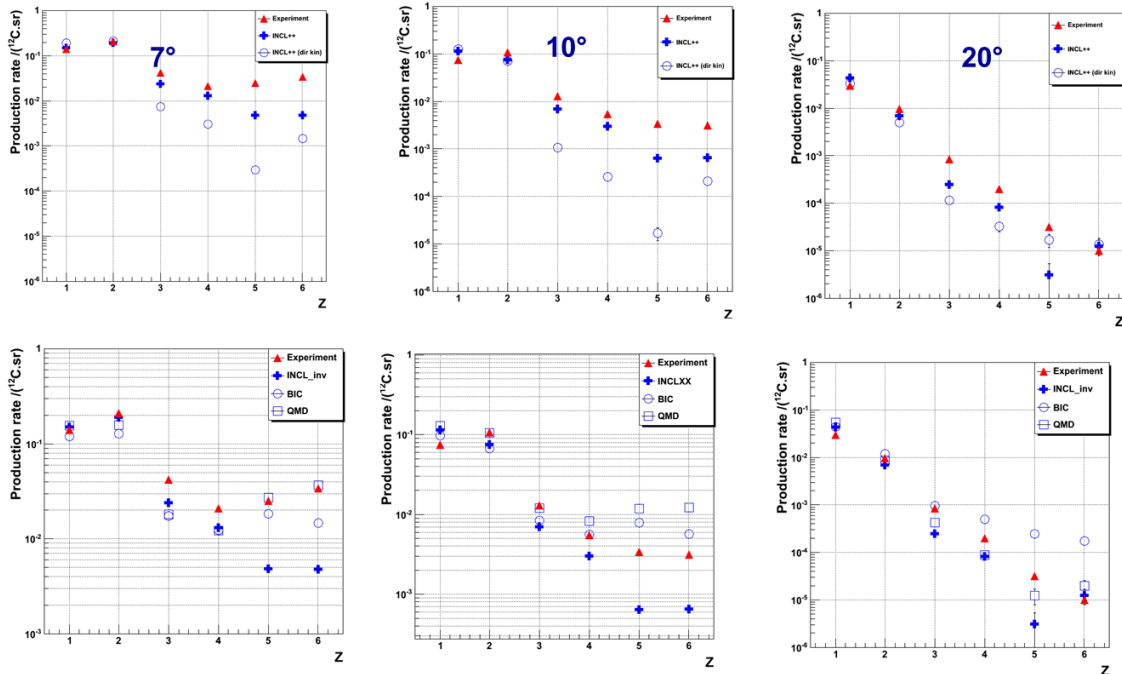
Conclusions

We have presented in this paper the new capabilities of the Liège Intranuclear Cascade model, INCL4, which is now implemented into several high-energy transport codes. This allows the simulation of spallation targets. The example of the European Spallation Source (ESS) tungsten target was shown, for which a careful benchmarking of the code on W elementary cross-sections (excitation functions) allows assessing the uncertainty on the predictions of the most hazardous isotopes.

A study of the production of astatine (Z=85) isotopes in the ISOLDE (CERN) lead-bismuth target shows that our model, thanks to the coalescence mechanism in the intranuclear cascade model and to an improved handling of low energy helium-induced reactions, correctly reproduces the measured astatine yields. More generally, this indicates that it is well suited for predicting isotopes generated in secondary reactions.

The recent extension of the model to light ion induced reactions was also discussed. Although the treatment of target and projectile is not fully symmetric, but provided that the model is used with the kinematics (direct or inverse) most appropriate to the considered observables, it gives very satisfactory results when compared to different sets of experimental data. Being included in GEANT4, it can be used to simulate thick target problem and gives results generally better than BIC and comparable or only slightly less good than QMD, but with a much shorter CPU time. Further improvements, in particular to make the model symmetrical for projectile and target, are under progress.

An extension to energies up to 10 GeV, which requests the adding of multipion [28] and strangeness production channels, is under also progress.

References

[1]   Boudard, A. *et al.*, *Phys. Rev. C* 66, 044615 (2002).

[2]   Junghans, A.R. *et al., Nucl. Phys. A*, 629 (1998) pp. 635-655.

[3]   HINDAS. EC contract FIKW-CT-2000-00031, Final report. ed. J.P. Meulders, A. Koning and S. Leray, 2005.

[4]   FP6 Euratom project EUROTRANS/NUDATRA, 2004 EC contract number FI6W-CT-2004-516520.

[5]   Boudard, A. and Cugnon, J,*, Proc. of the ICTP-IAEA Advanced Workshop on Model Codes for Spallation Reactions*, IAEA INDC(NDS)-0530, Vienna, August 2008, p. 29. http://www-nds.iaea.org/reports-new/indc-reports/indc-nds/indc-nds-0530.pdf

[6]   Kelić, A. *et al., Proc. of the ICTP-IAEA Advanced Workshop on Model Codes for Spallation Reactions*, IAEA INDC(NDS)-0530, Vienna, August 2008, p. 181

[7]   David, J.C. *et al., Shielding Aspects of Accelerators, Targets and Irradiation Facilities - SATIF 10 Workshop Proceedings*, Geneva, Switzerland 2-4 June 2010, p. 273.

[8]   Leray, S. *et al., Journal of the Korean Physical Society*, Vol. 59, No. 2, August 2011, p. 791

[9]   http:/www-nds.iaea.org/spallation.

[10]   Boudard, A. *et al., accepted for publication in Phys. Rev. C*.

[11]   Niita, K. *et al.,* JAEA-Data/Code 2010-022 (2010)

[12]   Pelowitz, D. B. *et al.,* MCNPX 2.7.B extensions, Los Alamos Report LA-UR-09-04130 (2009)..

[13]   Agostinelli, S. *et al., Nucl. Instrum. Meth. A* 506 (2003) 250 – 303.

[14]   Leprince, A. *et al., Proceedings of the ICRS12 conference*, Nara, Sept. 2-7, 2012.

[15]   Ene, D. ESS Proposal for the source term definitions nuclides break down lists, private communication (2011).

[16]   Tall, Y. *et al., Proceedings of the International Conference on Nuclear Data for Science and Technology,* April 22-27, 2007, Nice, France, Ed. O. Bersillon, F. Gunsing, E. Bauge, R. Jacqmin, and S. Leray, EDP Sciences, 2008, p1069.

[17]   David, J.C. *et al., Proceedings of the ICRS12 conference*, Nara, Sept. 2-7, 2012; David, J.C. *et al., to be published.*

[18]   Mashnik, S.G. *et al., J. Phys.: Conf. Ser. 41 (2006) 340. Conf. on Physics of Reactors (PHYSOR96)*, Mito, Japan, Sept. 16-20, 1996, (1996) pp. E161.

[19]   A. Boudard, *et al., Proc. Int. Topical Meeting on Nuclear Research Applications and Utilization of Accelerators 2009*, Vienna, Austria, May 5-8, 2009.

[20]   Kaitaniemi, P. *et al., Progress in NUCLEAR SCIENCE and TECHNOLOGY*, Vol. 2 (2011) pp.788.

[21]   Heikkinen, A., Kaitaniemi, P., Boudard, A. *J. Phys. Conf. Ser.,* 119 (2008) 032024.

[22]   Quesada, J.M. *et al., 2011 Progress in NUCLEAR SCIENCE and TECHNOLOGY*, Vol. 2, pp.936-941.

[23]   Folger, G., Ivanchenko, V. N. and Wellisch, J. P. *Eur. Phys. J. A* 21(3) (2004) 407–417

[24]   Koi, T. *Proc. IEEE 2008 Nuclear Science Symposium,* Dresden, Germany, Oct. 19-25, 2008.

[25]   Iwata, Y. *et al., Phys. Rev.* C 64 (2001) 034607.

[26]   Zeitlin, C. *et al., 2008 Phys. Rev.* C 77 (2008) 034605.

[27]   Braunn, B. *et al., Nucl. Instrum. Meth.* B 269 (2011) 2676

[28]   Pedoux, S. *et al., Nucl. Instrum. Meth.* B 269 (2011) 2676